The Interdependence of the Degree of Precipitation and Dislocation Density during the Thermomechanical Treatment of Microalloyed Niobium Steel

Rešković, Stoja; Slokar Benić, Ljerka; Lovrenić-Jugović, Martina

Source / Izvornik: **Metals, 2020, 10, 1 - 11**

Journal article, Published version
Rad u časopisu, Objavljena verzija rada (izdavačev PDF)

https://doi.org/10.3390/met10020294

Permanent link / Trajna poveznica: https://urn.nsk.hr/urn:nbn:hr:115:053240

Rights / Prava: In copyright / Zaštićeno autorskim pravom.

Download date / Datum preuzimanja: **2024-04-27**

SVEUČILIŠTE U ZAGREBU METALURŠKI FAKULTET
UNIVERSITY OF ZAGREB FACULTY OF METALLURGY
SISAK

Repository / Repozitorij:

Repository of Faculty of Metallurgy University of Zagreb - Repository of Faculty of Metallurgy University of Zagreb

DIGITALNI AKADEMSKI ARHIVI I REPOZITORIJI

metals

MDPI

Article

The Interdependence of the Degree of Precipitation and Dislocation Density during the Thermomechanical Treatment of Microalloyed Niobium Steel

Stoja Rešković, Ljerka Slokar Benić * and Martina Lovrenić-Jugović

Faculty of Metallurgy, University of Zagreb, Aleja narodnih heroja 3, 44000 Sisak, Croatia; reskovic@simet.unizg.hr (S.R.); mlovrenic@simet.unizg.hr (M.L.-J.)

* Correspondence: slokar@simet.unizg.hr; Tel.: +38-544533381

Received: 13 January 2020; Accepted: 20 February 2020; Published: 24 February 2020

Abstract: In this paper, thermomechanical processing of niobium microalloyed steel was performed with the purpose of determining the interaction between niobium precipitates and dislocations, as well as determining the influence of the temperature of final deformation on the degree of precipitation and dislocation density. Two variants of thermomechanical processing with different final rolling temperatures were carried out. Samples were studied using electrochemical isolation with an atomic absorption spectrometer, transmission electron microscopy, X-ray diffraction analysis, and universal tensile testing with a thermographic camera. The results show that the increase in the density of dislocations before the onset of intense precipitation is insignificant because the recrystallization process takes place simultaneously. It increases with the onset of strain-induced precipitation. In this paper, it is shown that niobium precipitates determine the density of dislocations. The appearance of Lüders bands was noticed as a consequence of the interaction between niobium precipitates and dislocations during the subsequent cold deformation. In both variants of the industrial process performed on the cold deformed strip, Lüders bands appeared.

Keywords: niobium microalloyed steel; thermomechanical processing; deformation; precipitation; dislocation density; microstructure

1. Introduction

As a result of their wide range of industrial applications, microalloyed steels continue to be attractive and evoke significant interest. It is known that the mechanical properties of steel can be significantly improved by the addition of niobium because it retards austenite recrystallization and grain growth. At lower temperatures, niobium binds with free carbon and nitrogen in fine carbides or carbonitride precipitates, which inhibits austenite recovery and recrystallization. The final effect is to reduce the final ferrite grain size by increasing the density of ferrite nucleation sites [1].

The most cost-effective way of producing grain refinement, and thus improving the mechanical properties of steel, is thermomechanical controlled processing (TMCP), which in industrial practice involves the production of specific microstructures related to particular properties. TMCP for the improvement of the mechanical properties of microalloyed steels consists of controlled hot rolling followed by controlled cooling [2–4].

Microalloying technology and the thermomechanical treatment of microalloyed steels have evolved from theoretical knowledge of the mechanisms of precipitation hardening, grain size control, and steel deformation [5–7]. The processes of reinforcement and softening during the thermomechanical treatment of microalloyed steel and the formation of certain structures are related to the complex

interaction of the deformation, precipitation, and structure recrystallization processes [8]. These are temperature dependent, and the thermomechanical treatment of niobium microalloyed steel requires the careful selection of all process parameters. During the heating and steel austenitization stages, the heating temperature is very important. It is determined by the chemical composition of the steel and must ensure complete solubility of the niobium precipitates to provide sufficient niobium, carbon, and nitrogen content for precipitation during thermomechanical treatment [9,10]. A higher temperature than the complete solubility temperature of niobium carbonitride is not desirable because a longer austenitization time at high temperatures results in a heterogeneous increase in austenitic grains, resulting in poor mechanical and technological properties [8].

During the hot rolling process of Nb microalloyed steels, Nb (C,N) precipitates are formed as a result of Nb's strong affinity for bonding with C and N. These precipitates form an obstacle to the dislocations and austenite grain boundary movements and can provide precipitation strengthening. Here, it should be noted that the value of niobium as a microalloying element arises from its ability to generate sufficiently large pinning forces to retard the motion of dislocations and subgrain and grain boundaries during recovery and recrystallization [11–16].

In pre-deformation, which takes place at temperatures above 1000 °C, a high degree of deformation is achieved [1,4,7]. As a result of the high degree of deformation and high temperature, both static and dynamic recrystallizations take place completely. Heterogeneously distributed larger precipitates, mainly niobium nitrides, are present in the steel. At this stage of thermomechanical processing, both static and dynamic recrystallization are present and significant austenitic grain refinement is achieved. In the final stage of thermomechanical processing, which takes place after pre-deformation and must finish before the phase transformation of steel, the deformation, recrystallization, and precipitation processes take place. They are interdependent, and their dependence is very complex. Strain-induced precipitation (SIP) plays the largest role. The resulting precipitates are very small, up to 8 nanometers in size, and are precipitated in the form of close-packed rows. It was proven that the start of strain-induced precipitation depends on the temperature, degree of deformation, and content of niobium, the microalloying element [9,15,17]. Strain-induced precipitates are a strong obstruction to the movement of dislocations during plastic flow. Dislocations accumulate around the precipitates, forming subgrains that represent the nuclei of new grains in the process of recrystallizing. The higher density of dislocations inhibits and ultimately stops dynamic recrystallization [18]. At the end of the final deformation, which has a small degree of deformation in the final passes, high stresses are present in the structure as a result of the high density of dislocations. Phase transformation of such structures results in a fine-grained ferrite–pearlite structure with homogeneous and high mechanical properties.

As a result of the high density of dislocations, a fine-grained structure is obtained after phase transformation. The cooling rate has a significant impact on grain size [16,19,20]. At this stage of thermomechanical processing, a $\gamma \rightarrow \alpha$ phase transformation takes place. Higher cooling rates imply a greater proportion of carbide phases in the structure.

Subsequent cold deformation of the hot rolled strip of niobium microalloyed steel may cause Lüders bands to appear [19,20]. This phenomenon has been intensively investigated over the last 7–8 years. The findings to date show that the appearance of Lüders bands is related to an atmosphere of niobium precipitates and of carbon and nitrogen atoms. Investigations into the appearance of Lüders bands in niobium microalloyed steels showed that it is related with the degree of niobium bonding in precipitates, the size of these precipitates, and with interactions with dislocations. It was proven that in steels containing niobium precipitates larger than 40 nm during cold deformation, Lüders bands do not appear [19,20]. The degree of precipitation depends on the temperature rolling mode of the strip. On the other hand, when the degree of precipitation is high, a large number of tiny, strain-induced precipitates occur, which represent strong obstacles to the movement of dislocations [21,22].

The aim of this study is to determine the influence of the final deformation parameters on the degree of precipitation of niobium carbonitride and the appearance of Lüders bands. Therefore,

two thermomechanical processing schedules with different final rolling temperatures were performed. The change in dislocation density was investigated in detail through each step of TMCP, as well as its correlation with deformation and the degree of precipitation. Finally, the appearance of Lüders bands for both variants was investigated.

2. Materials and Methods

Low-carbon steel with a chemical composition of 0.12% C, 0.78% Mn, 0.18% Si, 0.020% Al, 0.0011% P, 0.018% S, and 0.0079% N microalloyed with 0.048% Nb was selected for this study. Two variants of industrial thermomechanical processing were implemented: high temperature (HT), in which the start of the final deformation occurred at 1020 °C, and low temperature (LT), in which the start of the final deformation occurred at 987 °C. The heating and austenitization were performed at 1250 °C for 3.1 h. The pre-deformation was carried out in the temperature range 1180–1040 °C with a total reduction of 92.25%.

Austenitizing and pre-deformation were completely identical in both variants. The degrees of deformation in all passes of the final deformation were also almost identical. In the LT variant, the final deformation was performed in the temperature range 987–887 °C, with five passes resulting in a total reduction of 83.10%. In the HT variant, the final deformation was also performed with five passes resulting in a total reduction of 82.98%, but in the temperature range 1020–905 °C. The strip was cooled to 560 °C and reeled. The temperature was measured using an optical pyrometer. A schematic of the final deformation is shown in Figure 1.

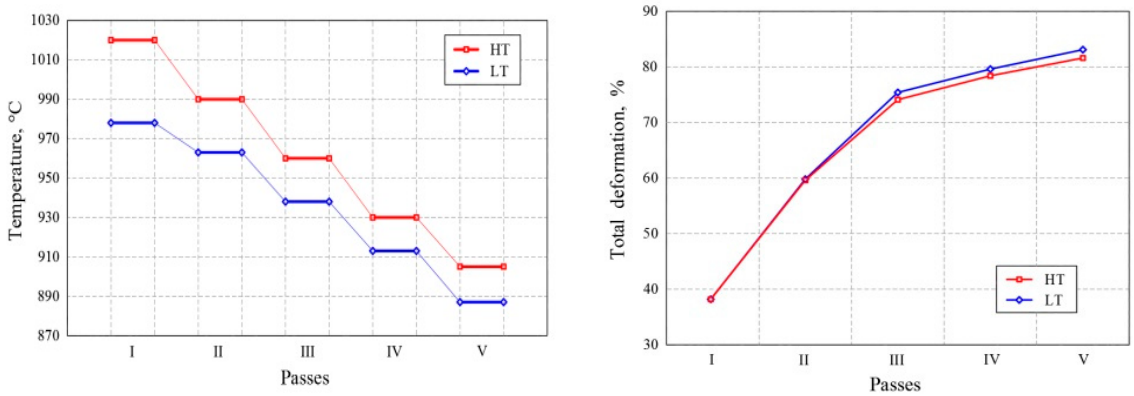

Figure 1. (**a**) Schematic of the final deformation (FD) and (**b**) the change in the degree of deformation.

Samples for testing were taken at characteristic spots from each phase of thermomechanical treatment. Sampling was carried out in such a way that the strip was stopped at a chosen moment. Then, the samples of interest from the deformation zone and its vicinity were rapidly cooled by applying the maximum amount of cooling water onto the rollers. In this way, the structural development and the processes involved in each phase of thermomechanical finishing were blocked. Reductions in the samples were determined using various methods of analysis. For electrochemical isolation, samples in the form of a plate with dimensions 80 mm × 20 mm were electrolytically dissolved in a cell according to the method described by W. Koch [23]. The isolate was identified using an atomic absorption spectrophotometer (AAS, Perkin Elmer, Waltham, MA, USA). The size and distribution of niobium precipitates, as well as their interaction with dislocations, were analyzed using a transmission electron microscope (TEM, JEOL-2000, Tokyo, Japan). For analysis by TEM, samples were prepared using the foil method. For that purpose, samples in the form of a cylinder with a diameter of 3 mm were used. They were mechanically ground on 600 and 1000 grit papers and then electrolytically thinned to a fully transparent foil. Electrolytical thinning was performed in a solution of 5% $HClO_4$ and 95% CH_3COOH using a voltage of 45 V at room temperature. The samples prepared in this way were analyzed using

a transmission electron microscope at magnifications of 5000× and 200,000× and voltage of 200 kV. To determine the internal stresses in the material and the dislocation density, the X-ray diffraction method was used. Analyses were performed using a universal camera, a vertical diffractometer with Bragg–Brentano's focusing, and a graphite monochromator using Co Kα radiation (λ = 1.790 Å). Samples with dimensions 10 mm × 10 mm were analyzed after metallographic preparation by grinding, polishing, and deep etching. The diffraction line profiles were analyzed quantitatively by measuring the width at half the height of the maximum of the reflexes (110), (200), and (211) [24–26], while the dislocation density was calculated according to Smallman and Westmacott [27]:

$$\varphi = \frac{3}{D^2} \left(\mathrm{m}^{-2}\right) \quad (1)$$

where D is the subgrain size [10]. The microstructure of metallographically prepared samples after etching in nital was observed using a light microscope (Leitz Ortholux, Wetzlar, Germany), and images were taken using an Olympus digital camera. The appearance and propagation of the Lüders bands were analyzed by tensile testing, up to breaking point, on a Zwick 50 kN universal tensile testing machine (Zwick, Ulm, Germany). Simultaneous measurements of the temperature change in the deformation zone were taken using a VarioCAM M82910 thermographic camera (Jenoptik, Jena, Germany) with a temperature sensitivity of 80 mK. The measured results were analyzed using Irbis professional software (InfraTec GmbH, Dresden, Germany).

3. Results and Discussion

Figure 2 shows that in the pre-deformation in both variants, the degree of precipitation was low (11.8–12.1%) and did not change significantly from the onset to the end of pre-deformation. In the final deformation, there was an increase in the degree of precipitation in both variants. Nevertheless, it was slightly lower in the HT variant (25%) than in the LT variant (26%). The precipitation continued during the cooling phase of the strip and was higher for the high temperature variant (36.5%) as compared to low temperature variant (34%). Since in both variants the steels were heated under the same conditions to the same temperature (1250 °C), it was assumed that the achieved solubility of niobium was the same in both variants.

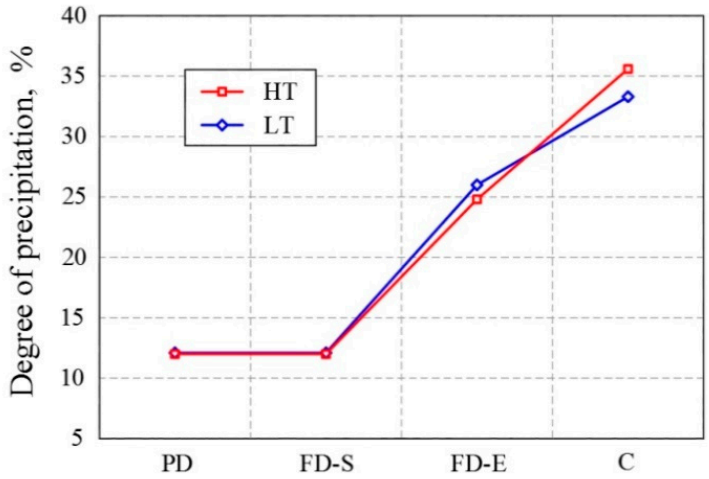

Figure 2. Degree of precipitation of niobium in each stage of thermomechanical processing. (PD: pre-deformation, FD-S: final deformation—start, FD-E: final deformation—end, C: cooling).

Transmission electron analysis of the pre-deformed samples showed niobium precipitates (Figure 3). These precipitates were coarse, of spherical shape, and larger than 20 nanometers and were heterogeneously distributed in structure.

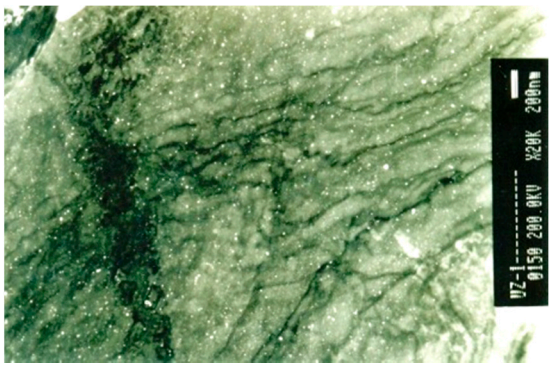

Figure 3. TEM micrograph of niobium precipitates in pre-deformation, reproduced from [10], with permission from Taylor&Francis, 2013.

In principle, precipitation of Nb carbides can occur in austenite or ferrite on grain boundaries, dislocations, subgrain boundaries, or interphase boundaries during the austenite-to-ferrite transformation [28].

In the final phase of thermomechanical treatment in both variants, the samples were examined after each pass (Figure 4a). The degree of precipitation in the HT variant was lower than that in the LT variant, and for the first three passes, they remained low and were similar for both variants (11.8–12.1%).

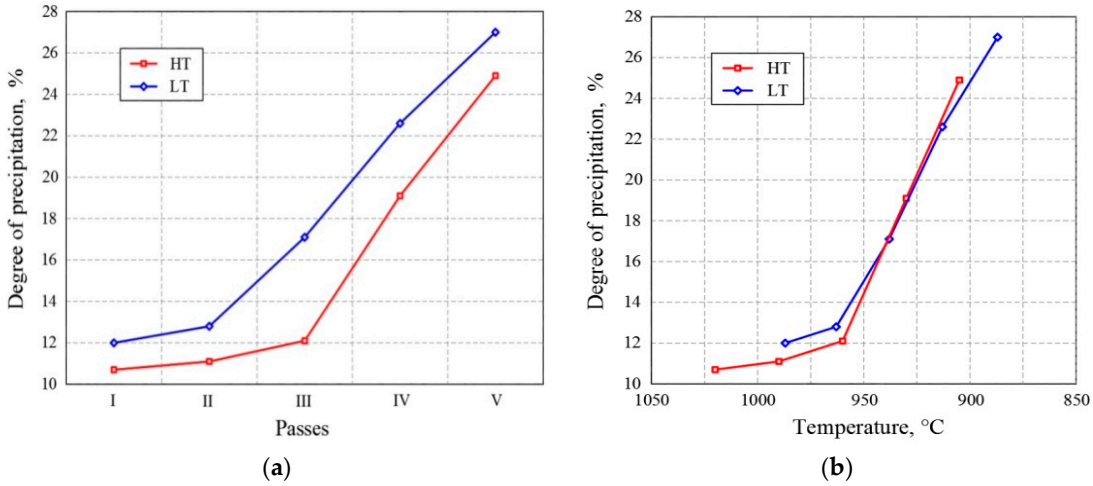

Figure 4. Change in precipitation degree (**a**) through passes and (**b**) with the temperature of thermomechanical processing.

Although it is known from the literature [29–31] that strain-induced precipitation is a function of temperature, deformation, and time, the results obtained in this study (shown in Figure 4) imply that SIP is more temperature dependent. In particular, in the low temperature variant, intensive, strain-induced precipitation started after the second pass (at 963 °C). In the high temperature variant, strain-induced precipitation began after the third pass (at 960 °C). Figure 4b clearly shows that the onset of intense strain-induced precipitation is more temperature dependent than the degree of deformation (Figure 4a). Strain-induced precipitation begins at a temperature of about 960 °C. It was found that, until the onset of strain-induced precipitation in both variants, dynamic and static recrystallization proceeded undisturbed. This is very important in the sense of the determination of hot rolling parameters. At 930 °C, the degree of precipitation was the same in both variants. In the fourth pass and in the fifth pass, there were significant increases in the degree of precipitation, amounting to 19% and 25%, respectively. Figure 4b clearly shows that with the decrease in temperature, the degree of precipitation increased in the LT as well as in the HT variant.

The beginning of strain-induced precipitation was also confirmed by transmission electron microanalysis (Figure 5). The strain-induced precipitates were very small, below 10 nanometers, and arranged in rows. The fraction of strain-induced precipitates and their average size are directly influenced by the amount of deformation [32].

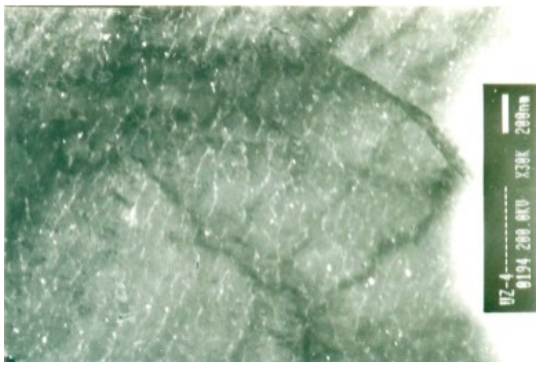

Figure 5. TEM micrograph showing the onset of strain-induced precipitation at 963 °C, low temperature (LT) variant.

In the last passes of the final thermomechanical processing in both variants, the degree of total deformation decreases (Figure 6) while dislocation density increases, as is the case with the degree of precipitation (Figure 4a). In investigations of the same steels [10] it was proven that the low temperature rolling schedule leads to considerably higher rolling forces in the last three passes.

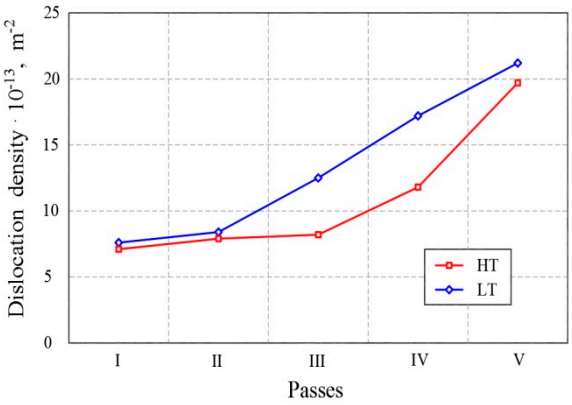

Figure 6. Change in the dislocation density by stages of final thermomechanical processing.

In order to determine the quantitative amount of changes in the structure, a study of the diffraction line profile was carried out. By studying the diffraction line profile in each pass of the HT and LT thermomechanical processing, a significant difference was observed both from the beginning to the end of the thermomechanical process and in each pass in both variants. From the profile of diffraction lines, the density of dislocations, ϕ (m^{-2}), was calculated according to Equation (1).

The onset of strain-induced precipitation depended on the temperature, as is shown in Figure 7. In the first two passes, the degree of deformation was high and almost identical for both variants. Static and dynamic recrystallization took place undisturbed, so the dislocation density was lower. When strain-induced precipitation began at 960 °C, the recrystallization became inhibited and the dislocation density increased. In the last passes, the degree of deformation was small, but the density of dislocations increased as the degree of precipitation increased. Precipitates arranged in close-packed arrays became a strong obstacle to the movement of dislocations. Therefore, dislocations became immobile and their density increased.

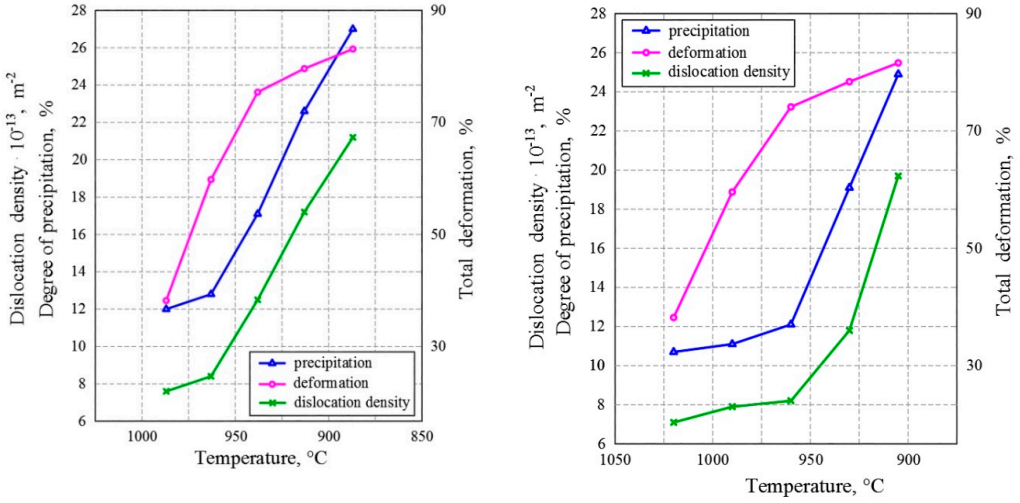

Figure 7. Relation between the degree of precipitation, the dislocation density, and temperature for (**a**) the LT variant and (**b**) the HT variant.

Figure 7a shows that in the LT variant, the degree of precipitation almost linearly increased with the decrease in temperature after two passes. Dislocation density at the onset of deformation increased, but after the third pass, there was an evident slowdown, as can be seen in the values. Figure 7b shows similar tendencies for the HT variant, with the only difference being that a significant increase in the degree of precipitation and deformation occurred after the third pass. Further, it can be clearly seen that a change in the density of dislocations was associated with a change in the degree of precipitation. At the beginning of strain-induced precipitation, interaction of the precipitate and dislocations occurred and the dislocation density increased, as is shown in Figure 8.

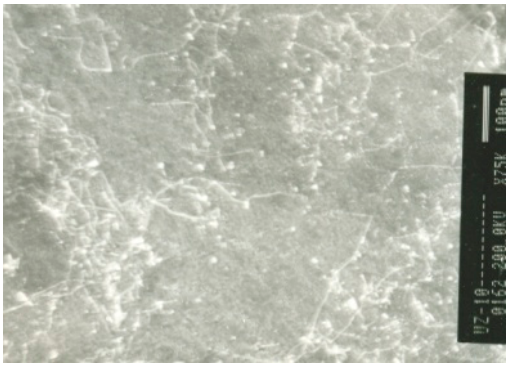

Figure 8. TEM micrograph of the interaction between precipitates and dislocations [20].

After the third pass, the major influence on the dislocation density was shown to be the degree of precipitation rather than the degree of deformation. Specifically, in microalloyed steels, recrystallization and precipitation can interact in at least three distinct ways [2]. Firstly, a decrease in dislocation density through recrystallization reduces the number of precipitate nucleation sites available and can thus retard the onset and rate of precipitation; this occurs after the onset of intense deformation-induced precipitation (960 °C) and is evident in the first two passes in the LT variant, as well as in the first three passes in the HT variant. Secondly, precipitate dispersion can provide a pinning (Zener) force that can retard or halt the progress of recrystallization; this is evident in the latest passes of final TMCP, because by increasing the degree of precipitation, the density of blocked dislocations also increases, as shown in Figure 7. Precipitates are arranged in rows at the onset of SIP (Figure 5), but after it, they are dispersed, accumulating in certain places and blocking the dislocations (Figure 8).

Thirdly, the mobility of grain boundaries is strongly affected by the solute content of the matrix and its diffusivity. Particularly, the diffusivity of Nb is an important factor contributing to the significant retarding effect on recovery and recrystallization; it slows down boundary motion since it interacts with the boundary and does not diffuse rapidly enough to keep up with the migrating boundary. The higher degree of precipitation leads to the decrease in the amount of free Nb that can diffuse. Furthermore, as a result of the larger atomic radius of Nb than those of carbon, nitrogen, and iron, Nb moves more slowly; thus, it cannot track the grain boundary, and its diffusivity decreases. Further, the dislocation density increases even though the energy of the system and the temperature decrease, and so the total deformation slows down. Therefore, close-packed carbonitride rows and interaction between precipitates and dislocations are present in the structure (Figure 9). The further increase in deformation and precipitation also increases the density of dislocations, as was also observed in [18]. Dislocations pile up on rows of precipitates and form the boundary of the subgrain (Figure 9).

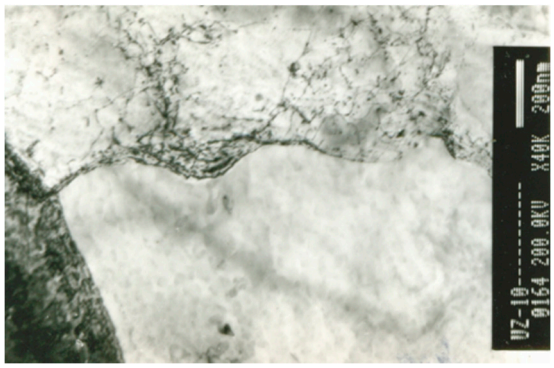

Figure 9. TEM micrograph of dislocations accumulating on the rows of precipitations.

In the last passes, the recrystallization and recovery mechanisms were halted and completely stopped. Specifically, fine precipitates pinned dislocations and thus retarded recovery. In such conditions, further deformation leads to an increase in the density of dislocations.

Before the phase transformation, there was enough solute niobium present in the steel to delay the transformation. Specifically, solute niobium delays transformation significantly, which lowers the temperature, resulting in a higher ferrite nucleation rate and lower ferrite growth rate. As the phase transformation takes place relatively slowly, there is a possibility for interphase precipitation. After slow cooling, which occurs in the air, there is a chance for spontaneous precipitation [33]. In this study, it was found that in the HT variant, precipitation of 36.5% was achieved, and in the LT variant, 34% was achieved. As a final step of TMCP, after rolling, both strips (the LT and HT variants) were cooled at the same speed. Precipitation continued, and these precipitates had a beneficial effect in preventing ferritic perlite grain growth. A fine-grained, ferrite–pearlite microstructure with almost the same grain size was achieved (Figure 10).

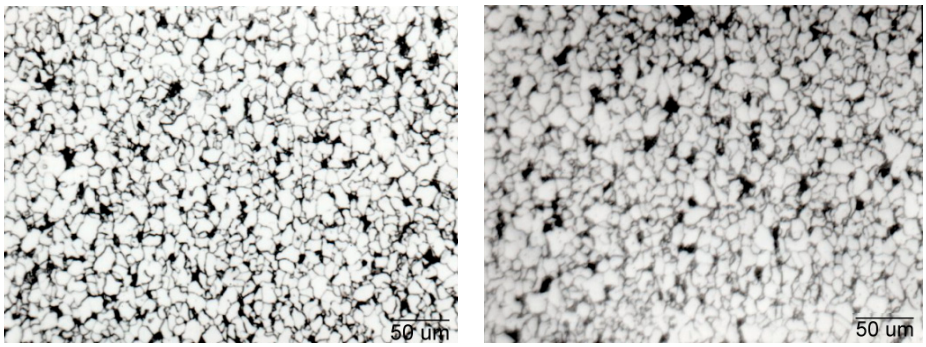

(**a**) (**b**)

Figure 10. Microstructure of the hot rolled strips of Nb microalloyed steel. (**a**) LT variant. (**b**) HT variant.

In both variants of TMCP, the precipitation of Nb, the interaction of precipitates, and dislocations resulted in a fine-grained, homogeneous structure. In the cooled strip, the degree of precipitation in the high temperature variant (36.5%) was higher as compared to that in the low temperature variant (34%). This indicates that the binding of niobium to precipitates (NbC, NbN, Nb(CN)) was not accomplished entirely. Free niobium may affect the appearance of Lüders bands. The dislocation density was about the same, 10^8 m^{-2}. Steels of similar chemical composition but not containing Nb have a dislocation density of 10^6 m^{-2}.

The subsequent cold deformation of the strip shows the appearance of inhomogeneous deformations at the beginning of the plastic flow of the material. These inhomogeneous deformations (stress–strain curve) are related to the appearance of Lüders bands (Figure 11). Specifically, Lüders bands are localized regions of plastic deformation that are often observed in cold-rolled low-carbon steel following the appearance after the limit of proportionality [34–39].

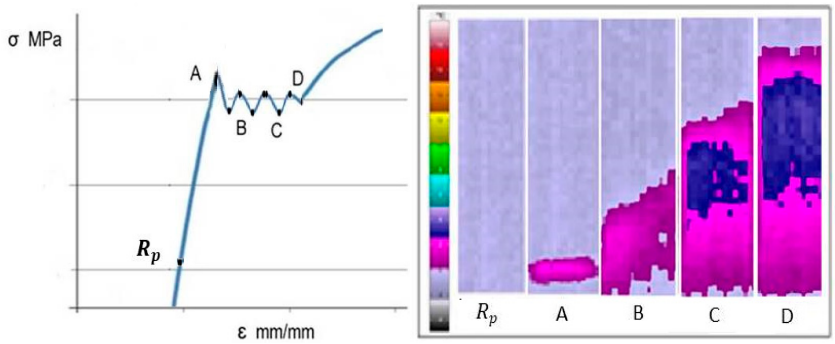

Figure 11. The stress–strain curve and distribution of temperature change at the beginning of the plastic material flow in the field of the appearance of Lüders bands.

When the interaction energy between dislocations and easily diffused solute atoms (C, N, and Nb) is strong, they gather around dislocations to form Cottrell's atmospheres. Then, dislocations are strongly anchored and the stored energy of the dislocation is decreased. When the upper yield point is reached in cold deformation, the number of moving dislocations increases because of the formation of new dislocations as a result of the multiplication mechanism. Moving dislocations are formed only at the places of the highest stress concentration. This moment corresponds to the development of Lüders bands. The appearance of Lüders bands was observed in both variants [34,37] as a consequence of the interaction between niobium strain-induced precipitates and dislocations during cold deformation [36].

4. Conclusions

Research conducted within the framework of this paper resulted in the following conclusions:

- During the final thermomechanical processing of niobium microalloyed steel, the onset of deformation-induced precipitation begins at 960–963 °C. Precipitation is continuous during the final deformation phase and during the cooling period. At the end, a significant amount of free niobium remained in both variants;
- The increase in the density of dislocations before the onset of intense precipitation is insignificant because in the material, in addition to deformation, recrystallization and recovery occur;
- With the onset of strain-induced precipitation, the density of dislocations increases. This indicates that the recrystallization and recovery mechanisms are slowing down or are completely absent, with further deformation and precipitation being caused by the niobium content. As the degree of niobium strain-induced precipitation increases, the density of dislocations also increases.

Finally, niobium precipitates determine the density of dislocations. The interaction of niobium precipitations and dislocations, as well as free niobium, carbon, and nitrogen, could be related to the inhomogeneous deformations that are associated with the appearance of Lüders bands

Author Contributions: Conceptualization, S.R.; methodology, S.R.; software, M.L.-J.; validation, S.R.; formal analysis, L.S.B. and M.L.-J.; investigation, L.S.B.; resources, S.R.; writing—original draft preparation, S.R. L.S.B. and M.L.-J.; writing—review and editing, S.R. and L.S.B.; visualization, M.L.-J.; supervision, S.R.; project administration, S.R.; funding acquisition, S.R. All authors have read and agreed to the published version of the manuscript.

Funding: This was funded by Croatian Science Foundation under Project Number IP-2016-06-1270, Principal investigator: S.R.

Acknowledgments: Special thanks to F. Vodopivec and V. Novosel-Radović for significant contributions to this research.

Conflicts of Interest: The authors declare no conflict of interest.

References

1. Perez, M.; Courtois, E.; Acevedo, D.; Epicier, T.; Maugis, P. Precipitation of niobium carbonitrides in ferrite: Chemical composition measurements and thermodynamic modeling. *Philos. Mag. Lett.* **2007**, *87*, 645–656. [CrossRef]
2. Vervynckt, S.; Verbeken, K.; Lopez, B.; Jonas, J.J. Modern HSLA steels and role of non-recrystallisation temperature. *Int. Mater. Rev.* **2012**, *57*, 187–207. [CrossRef]
3. Baker, T.N. Microalloyed steels. *Ironmak. Steelmak.* **2016**, *43*, 264–307. [CrossRef]
4. Gong, P.; Palmiere, E.J.; Rainforth, W.M. Dissolution and precipitation behaviour in steels microalloyed with niobium during thermomechanical processing. *Acta Mater.* **2015**, *97*, 392–403. [CrossRef]
5. DeArdo, A.J. Metallurgical basis for thermomechanical processing of microalloyed steels. *Ironmak. Steelmak.* **2001**, *28*, 138–144. [CrossRef]
6. Pickering, F.B. The spectrum of microalloyed high strength low alloyed steels. In *HSLA Steels, Technology and Applications, Proceedings of the International Conference on Technology and Applications of HSLA Steels, Philadelphia, PA, USA, 3–6 October 1983*; American Society for Metals: Metals Park, OH, USA, 1984; p. 234.
7. Roberts, W. Recent innovations in alloy design and processing of microalloyed steels. In *HSLA Steels, Technology and Applications, Proceedings of the International Conference on Technology and Applications of HSLA Steels, Philadelphia, PA, USA, 3–6 October 1983*; American Society for Metals: Metals Park, OH, USA, 1984; p. 33.
8. Tanaka, T.; Tabata, N.; Hatamura, T. There stages of the controlled rolling process. In *Microalloying 75*; Union Carbide Corporation: New York, NY, USA, 1977; p. 75.
9. Honeycombe, R.W.K. Fundamental aspects of precipitation in microalloyed steels. In *HSLA Steels, Technology and Applications, Proceedings of the International Conference on Tehnology and Aplications of HSLA Steels, Philadelphia, PA, USA, 3–6 October 1983*; American Society for Metals: Metals Park, OH, USA, 1984; p. 243.
10. Vodopivec, F.; Rešković, S.; Mamuzić, I. Evolution of substructure during continuous rolling of microalloyed steel strip. *Mater. Sci. Technol.* **1999**, *15*, 1293–1299. [CrossRef]
11. Tirumalasetty, G.K.; van Huis, M.A.; Fang, C.M.; Xu, Q.; Tichelaar, F.D.; Hanlon, D.N.; Sietsma, J.; Zandbergen, H.W. Characterization of NbC and (Nb,Ti)N nanoprecipitates in TRIP assisted multiphase steels. *Acta Mater.* **2011**, *59*, 7406–7415. [CrossRef]
12. San Martin, D.; Caballero, F.G.; Capdevila, C.; de Andres, C.G. Discussion on the rate controlling process of coarsening of niobium carbonitrides in a niobium microalloyed steel. *Mater. Sci. Forum* **2005**, *500–501*, 703–710. [CrossRef]
13. Karmakar, A.; Biswas, S.; Mukherjee, S.; Chakrabarti, D.; Kumar, V. Effect of composition and thermo-mechanical processing schedule on the microstructure, precipitation and strengthening of Nb-microalloyed steel. *Mater. Sci. Eng. A Struct.* **2017**, *690*, 158–169. [CrossRef]
14. DeArdo, A.J. Niobium in modern steels. *Int. Mater. Rev.* **2003**, *48*, 371–402. [CrossRef]
15. Rešković, S. Studij Mehanizama Precipitacije i Rekristalizacije u Području Završnog Oblikovanja Mikrolegiranog Čelika. Ph.D. Thesis, Faculty of Metallurgy, University of Zagreb, Sisak, Croatia, 1997.
16. Rešković, S.; Vodopivec, F.; Mamuzić, I. Precipitation of Niobium in the final high—Temperature thermomechanical treatment. In Proceedings of the 4th International Conference on Production Engineering CIM '97, A-107, Opatija, Croatia, 12–13 June 1997; Croatian Association of Production Engineering: Zagreb, Croatia, 1997.
17. Hoogendoorn, T.M.; Spanraft, M.J. Quantifying the effect of microalloying elements on structures during processing. In *Microalloying 75*; Union Carbide Corporation: New York, NY, USA, 1977; p. 57.

18. Rešković, S.; Vodopivec, F.; Novosel-Radović, V.; Mamuzić, I. The influence of a hot plastic deformation on the crystal latice distortion change of a thermomechanical treatment microalloyed steel. In Proceedings of the 5th International Scientific Conference on Production Engineering CIM '99, Opatija, Croatia, 17–18 June 1999; Croatian Association of Production Engineering: Zagreb, Croatia, 1999; pp. 121–129.
19. Slokar Benić, L.; Rešković, S.; Marciuš, M.; Brlić, T. Change of microstructure of Nb microalloyed steel at start of the plastic flow during the cold deformation. In Proceedings of the 256th The IIER International Conference, Barcelona, Spain, 23–24 September 2019; IRAJ Research Forum: Bhubaneswar, India, 2019; pp. 17–19.
20. Rešković, S.; Jandrlić, I. Influence of Niobium on the beginning of the plastic flow of material during cold deformation. *Sci. World J.* **2013**, *2013*, 1–5. [CrossRef] [PubMed]
21. Han, J.; Lu, C.; Wu, B.; Li, J.; Li, H.; Lu, Y.; Gao, Q. Innovative analysis of Luders band behaviourin X80 pipeline steel. *Mater. Sci. Eng. A Struct.* **2017**, *683*, 123–128. [CrossRef]
22. Tovee, J.-P. Microstructural Influence on the Effects of Forward and Reverse Mechanical Deformation in HSLA X65 and X80 Linepipe Steels. Ph.D. Thesis, School of Engineering and Physical Sciences, University of Birmingham, Birmingham, UK, 2014.
23. Koch, W. Electrolytic Isolation of Carbide in Alloyed and Unalloyed Steels. *Stahl U.E.* **1949**, *69*, 69.
24. Warren, B.E.; Averbach, B.L. The separation of cold-work distortion and particle size broadening in X-ray patterns. *J. Appl. Phys.* **1952**, *23*, 497. [CrossRef]
25. Novosel-Radović, V.J. X-ray-difraction in laboratory of iron-steel and pipe works Sisak. *Strojarstvo* **1994**, *36*, 69–76.
26. Warren, E. *X-ray Diffraction*; Addison Wesley: Reading, MA, USA, 1969.
27. Smallman, R.E.; Westmacott, K.H. Stacking faults in face-centred cubic metals and alloys. *Philos. Mag.* **1957**, *2*, 669–683. [CrossRef]
28. Charleux, M.; Poole, W.J.; Militzer, M.; Deschamps, A. Precipitation behavior and its effect on strengthening of a HSLA-Nb/Ti steel. *Metall. Mater. Trans. A* **2001**, *32*, 1635–1647. [CrossRef]
29. Najafi-Zadeh, A.; Yue, S.; Jonas, J.J. Influence of hot strip rolling parameters on austenite recrystallization in interstitial free steels. *ISIJ Int.* **1992**, *32*, 213–221. [CrossRef]
30. Sakai, T.; Belyakov, A.; Kaibyshev, R.; Miura, H.; Jonas, J.J. Dynamic and post-dynamic recrystallization under hot, cold and severe plastic deformation conditions. *Prog. Mater. Sci.* **2014**, *60*, 130–207. [CrossRef]
31. Weiss, I.; Jonas, J.J. Interaction between recrystallization and precipitation during the high temperature deformation of HSLA steels. *Metall. Trans. A* **1979**, *10*, 831–840. [CrossRef]
32. Hutanu, R.; Clapham, L.; Rogge, R.B. Intergranular strain and texture in steel Luders bands. *Acta Mater.* **2005**, *53*, 3517–3524. [CrossRef]
33. Jia, T.; Militzer, M. The effect of solute Nb on the austenite-to-ferrite transformation. *Metall. Mater. Trans. A* **2015**, *46*, 614–621. [CrossRef]
34. Liss, R.B. Luder's bands. *Acta Metall.* **1957**, *5*, 341–342. [CrossRef]
35. Petit, J.; Wagner, D.; Ranc, N.; Montay, G.; Francois, M. Comparison of different techniques for the monitoring of the Lüders bands development. In Proceedings of the International Congress on Fracture, Bejing, China, 26–30 May 2013.
36. Rešković, S.; Brlić, T.; Jandrlić, I.; Vodopivec, F. Influence of strip cooling rate on Lüders bands appearance during subsequent cold deformation. In *New Technologies, Development and Application II*; Karabegović, I., Ed.; Springer: Cham, Switzerland, 2020; pp. 115–122.
37. Rešković, S.; Jandrlić, I.; Brlić, T. The influence of niobium content and initial microstructure of steel on the occurrence of Lüders band at the start of the plastic flow during cold deformation. *IOP Conf. Ser. Mater. Sci.* **2018**, *461*, 1–6. [CrossRef]
38. Brlić, T.; Rešković, S.; Jandrlić, I.; Skender, F. Influence of strain rate on stress changes during Lüders bands formation and propagation. *IOP Conf. Ser. Mater. Sci.* **2018**, *461*, 012007. [CrossRef]
39. Jandrlić, I.; Rešković, S.; Brlić, T. Distribution of stress in deformation zone of niobium microalloyed steel. *Metall. Mater. Int.* **2018**, *24*, 746–751. [CrossRef]

© 2020 by the authors. Licensee MDPI, Basel, Switzerland. This article is an open access article distributed under the terms and conditions of the Creative Commons Attribution (CC BY) license (http://creativecommons.org/licenses/by/4.0/).